Accepted Manuscript

Macrocyclic pyrrolobenzodiazepine dimers as antibody-drug conjugate payloads

Andrew F. Donnell, Yong Zhang, Erik M. Stang, Donna D. Wei, Andrew J. Tebben, Heidi L. Perez, Gretchen M. Schroeder, Chin Pan, Chetana Rao, Robert M. Borzilleri, Gregory D. Vite, Sanjeev Gangwar

PII: S0960-894X(17)31013-2
DOI: https://doi.org/10.1016/j.bmcl.2017.10.028
Reference: BMCL 25357

To appear in: *Bioorganic & Medicinal Chemistry Letters*

Received Date: 28 August 2017
Revised Date: 12 October 2017
Accepted Date: 14 October 2017

Please cite this article as: Donnell, A.F., Zhang, Y., Stang, E.M., Wei, D.D., Tebben, A.J., Perez, H.L., Schroeder, G.M., Pan, C., Rao, C., Borzilleri, R.M., Vite, G.D., Gangwar, S., Macrocyclic pyrrolobenzodiazepine dimers as antibody-drug conjugate payloads, *Bioorganic & Medicinal Chemistry Letters* (2017), doi: https://doi.org/10.1016/j.bmcl.2017.10.028

Graphical Abstract

To create your abstract, type over the instructions in the template box below.
Fonts or abstract dimensions should not be changed or altered.

Macrocyclic pyrrolobenzodiazepine dimers as antibody-drug conjugate payloads

Leave this area blank for abstract info.

Andrew F. Donnell, Yong Zhang, Erik M. Stang, Donna D. Wei, Andrew J. Tebben, Heidi L. Perez, Gretchen M. Schroeder, Chin Pan, Chetana Rao, Robert M. Borzilleri, Gregory D. Vite, and Sanjeev Gangwar

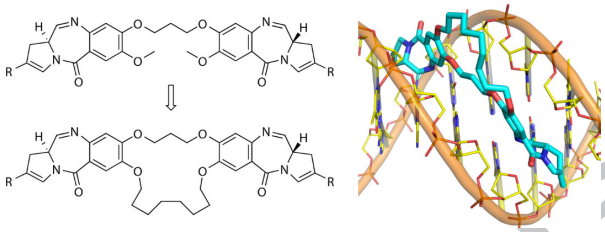

Bioorganic & Medicinal Chemistry Letters
journal homepage: www.elsevier.com

Macrocyclic pyrrolobenzodiazepine dimers as antibody-drug conjugate payloads

Andrew F. Donnell[a, *], Yong Zhang[a], Erik M. Stang[a], Donna D. Wei[a], Andrew J. Tebben[a], Heidi L. Perez[a], Gretchen M. Schroeder[a], Chin Pan[b], Chetana Rao[b], Robert M. Borzilleri[a], Gregory D. Vite[a], and Sanjeev Gangwar[b]

[a]*Bristol-Myers Squibb Research & Development, Princeton, NJ 08543, USA*
[b]*Bristol-Myers Squibb Research & Development, Redwood City, CA 94063, USA*

ARTICLE INFO

Article history:
Received
Revised
Accepted
Available online

Keywords:
Antibody-drug conjugates
Pyrrolobenzodiazepines
Macrocycles
Keyword_4
Keyword_5

ABSTRACT

Macrocyclic pyrrolobenzodiazepine dimers were designed and evaluated for use as antibody-drug conjugate payloads. Initial structure–activity exploration established that macrocyclization could increase the potency of PBD dimers compared with non-macrocyclic analogs. Further optimization overcame activity-limiting solubility issues, leading to compounds with highly potent (picomolar) activity against several cancer cell lines. High levels of in vitro potency and specificity were demonstrated with an anti-mesothelin conjugate.

* Corresponding author. Tel.: +1-609-252-5148; e-mail: andrew.donnell@bms.com

Cytotoxic drugs have been widely employed in cancer chemotherapy, but, in many cases, their therapeutic index is limited by adverse effects stemming from poor selectivity for cancer cells. Antibody-drug conjugates (ADCs) have the potential to mitigate these side-effects by harnessing the high specificity of antibodies to deliver small-molecule drugs directly to tumor cells.[1,2] Pyrrolobenzodiazepines (PBDs) are a family of sequence-selective DNA minor groove binding natural products whose potent cytotoxic properties make them attractive for use as ADC payloads.[3–5] PBD dimers such as **1** and **2**, formed by joining two PBD monomers via their C8-phenol groups with either a three-carbon or five-carbon spacer, inhibit a variety of cancer cell lines with subnanomolar IC_{50}s. Their high levels of activity have been attributed to an ability to promote intra- and interstrand DNA cross-linking by the formation of covalent aminal linkages between their reactive N10-C11 imine groups and the C2-NH_2 groups of guanine bases.[6] Interest in this class of compounds as ADC payloads is exemplified by vadastuximab talirine, an anti-CD33 conjugate of **1**, which has been advanced into clinic trials by Spirogen and Seattle Genetics.[7,8] Recently, an ADC based on **2** has also been described.[9] Both of these compounds employ a lysosomally-cleavable valine-alanine linker[10,11] for attachment of the payload to the antibody. In the case of **1**, the linker is attached directly to the aniline group. For **2**, the linker is attached to the N10-position of the hemiaminal form of **2** via a self-immolative *p*-aminobenzyl carbamate spacer.

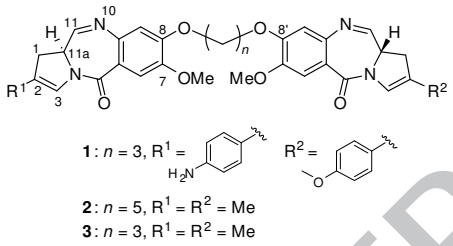

Our interest in these compounds was based on the examination of a model of PBD dimer **3** bound to DNA (Figure 1). The C11a-stereocenter imparts a conformation that is isohelical with the DNA minor groove, where the compound binds in a mode that enables the imine moieties to covalently bind the NH_2 groups of guanine bases on opposing strands. The C2-methyl groups project further along the groove, which is known to tolerate a variety of substituents, the nature of which can have a dramatic effect on the activity of the compounds.[12] This places the C7/C7'-methoxy groups in an exposed orientation, and we envisioned joining them with a linker to form macrocycles, potentially exploiting conformational restriction to improve potency. Modeling of a macrocyclic analog of **3** with a nine-carbon alkyl chain linking the phenols suggested that linkers of this length could be tolerated without distorting the helical binding geometry, although the ideal chain length was not apparent. Thus, as illustrated in Figure 2, our goals for SAR exploration were, first, to identify an appropriately-sized linker for macrocyclization, and, second, to match the macrocyclic PBD scaffold with suitable C2-substituents.

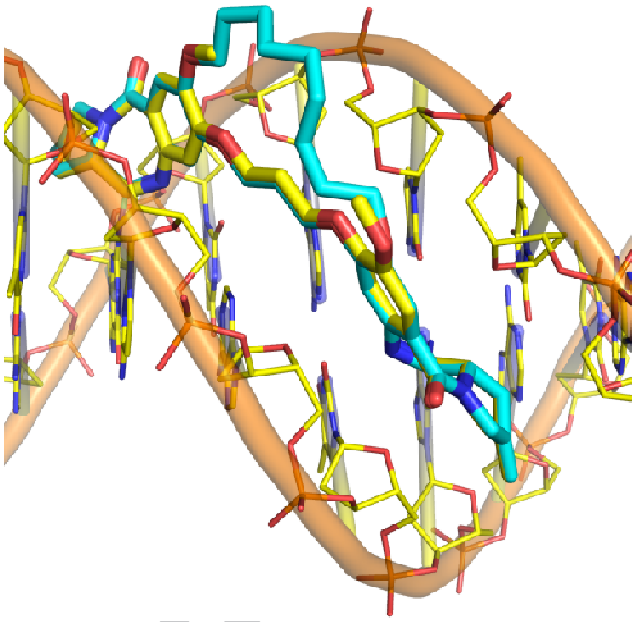

Figure 1. Model of PBD dimers bound to DNA. PBD dimer **3** is displayed in yellow and a macrocycle formed from **3** using a nine-carbon linker is displayed in cyan. Modeling was carried out using Maestro (Schrödinger, LLC, New York, NY) and the image was generated using PyMOL Molecular Graphics System (Schrödinger, LLC, New York, NY).

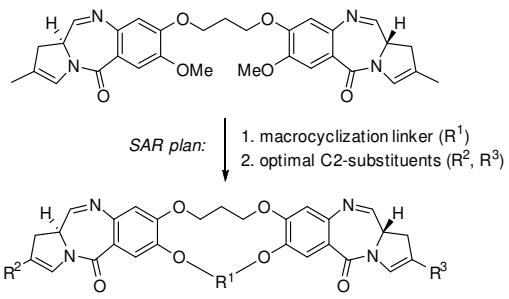

Figure 2. Areas for SAR exploration.

As an initial test of the tolerability of macrocyclization, we prepared a series of macrocyclic PBD analogs with alkyl linkers ranging in length from 7 to 12 carbons, giving 18- to 23-membered rings. While unsaturation and substitution at the C2-position of the PBD ring system are known to improve activity, we focused our early explorations on the more synthetically-tractable unsubstituted scaffold to establish the feasibility of macrocyclization as well as gain insight into the optimal ring size. We began by constructing the known PBD monomer **5** by adapting a reported five-step sequence starting from methyl 4-(benzyloxy)-5-methoxy-2-nitrobenzoate (**4**) (Scheme 1).[13] Dimerization was then effected by alkylation with 1,3-dibromopropane, and cleavage of the methyl ether groups revealed diphenol **6**.

We explored several routes for constructing macrocycles from **6**. Alkylation of the phenol groups with an appropriately-sized ω-bromo olefin set the stage for ring-closing metathesis, which proceeded in good yield but with by-products arising from olefin isomerization (this is illustrated in Scheme 2 for the compounds derived from 5-bromopent-1-ene). That proved useful at this stage, because we were able to carry the mixtures forward and isolate both the targeted species and its des-methylene congener

in sufficient quantities for initial biological evaluation. Compounds **8b–f** were made by this approach (see the Supplementary Data for the full experimental details). However, in many cases, isomer separation was challenging, and we felt that a more selective protocol would be needed to efficiently access larger quantities of material for analog synthesis. Some improvements in the RCM reaction were realized by carrying out the reaction in the presence of reported isomerization suppressors, such as 2,6-dichlorobenzoquinone,[14] although we did not fully optimize this approach because alternate methods for constructing the macrocyclic ring showed promise. For example, ring-closing alkyne metathesis was effective, but synthesis of the requisite internal alkyne precursors added to the overall complexity of the sequence. For many of the analogs, we relied on alkylation of **6** with a dihalo alkane, such as 1,7-dibromoheptane. This method was used to prepare compound **8a** and subsequent analogs. To complete the synthesis, the amide groups were converted to imines by a sequence involving N-alkylation with SEM-Cl, hydride reduction, and dehydration of the resultant hemiaminals by stirring with silica gel.[15]

To introduce C2-substitution and unsaturation, we used an alternate synthetic route where we first constructed the macrocyclic skeleton and then assembled the PBD ring system. This chemistry is illustrated in Scheme 3. Methyl 4-hydroxy-3-methoxybenzoate (**10**) was dimerized using 1,3-dibromopropane, and then nitration was followed by treatment with refluxing aqueous sodium hydroxide, which converted the methoxy groups to phenols with concomitant hydrolysis of the methyl esters. Re-esterification gave **11**, and alkylation with 1,8-diiodooctane provided the macrocycle **12**. Ester hydrolysis followed by coupling with the TBS-protected hydroxyproline derivative **13**[16] gave **14**. A one-pot nitro reduction/cyclization sequence forged the central ring of the PBD units, and protection of the resultant amide groups with SEMCl gave **15**. A three-step sequence converted the TBS ethers to alkenyl triflates **16**. From this intermediate, a variety of C2-substituents were installed using cross-coupling chemistry, and, finally, the imine moieties were unmasked to give the targeted compounds **17a–e**. Symmetrical homodimers **17a**-**b** were prepared from bis-triflate **16** by a Suzuki coupling with excess boronate (2.2 eq.). Heterodimers **17c–e** were constructed by first reacting **16** with 1 eq. of 4-aminophenylboronic acid pinacol ester and isolating the mono-arylated species from the resulting mixture, and then, in the case of **17c** and **17d**, installing the R^2 aryl group by a subsequent Suzuki coupling. Installation of a methyl group in **17e** was more effectively carried out by iron-catalyzed coupling with methyl magnesium bromide.

An analogous macrocycle with an ethylene glycol-based linker (**18**) was also prepared from **11** according to the same sequence, using 1,2-bis(2-iodoethoxy)ethane instead of 1,8-diiodooctane.

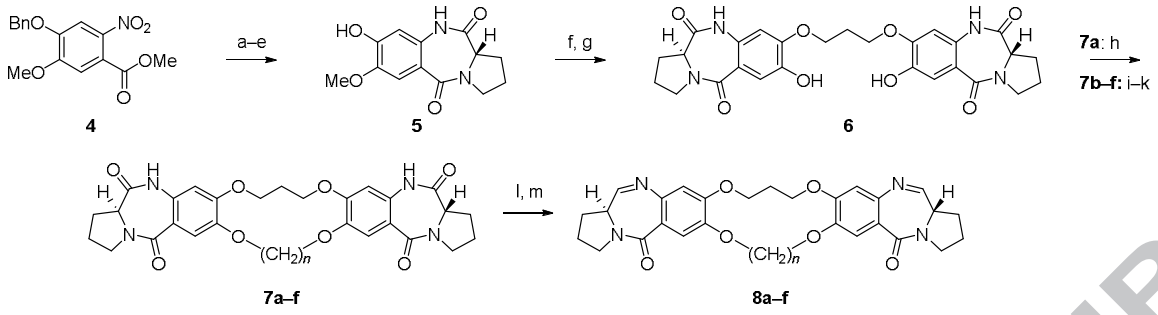

Scheme 1. Reagents and conditions: (a) 2.5 M aq. NaOH, THF, 50 °C, quant.; (b) $(COCl)_2$, DMF, THF, rt; (c) L-proline methyl ester hydrochloride, Et_3N, THF, 0 °C to rt, 72% (2 steps); (d) H_2 (50 psi), $Pd(OH)_2$, EtOH, rt; (e) AcOH, MeOH, 80 °C, 71% (2 steps); (f) 1,3-dibromopropane, K_2CO_3, DMSO, rt, 78%; (g) BBr_3, CH_2Cl_2, –78 °C to –5 °C, 33%; (h) 1,7-dibromoheptane, K_2CO_3, DMF, 50 °C; (i) for **7b**: 5-bromopent-1-ene; for **7c** and **7d**: 6-bromohex-1-ene; for **7e** and **7f**: 7-bromohept-1-ene, K_2CO_3, DMF, rt, 33–77% ; (j) Grubbs-II, DCE, 75 °C; (k) H_2, 10% Pd/C, MeOH, 64–88% of a mixture of two species (2 steps); (l) NaH, DMF, 0 °C; SEMCl; (m) $LiBH_4$, 1:1 THF–EtOH, 0 °C to rt; silica gel, 1:1 $CHCl_3$–EtOH, 4–37% (2 steps).

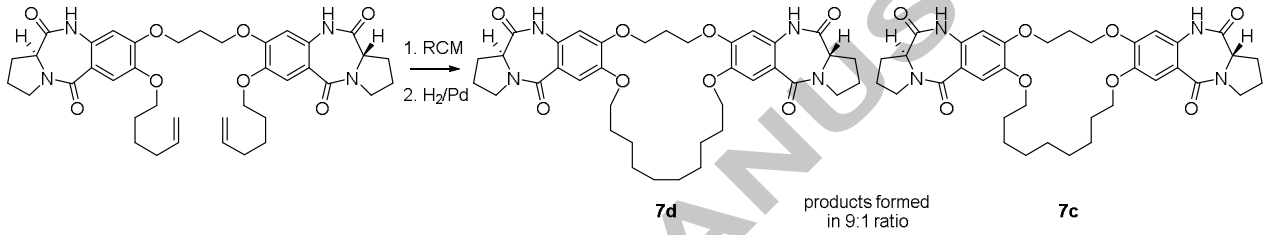

Scheme 2. Ring-closing metathesis proceeded with isomerization by-products. This is illustrated here using the pentene precursor, which gave rise to a mixture of **7d** and **7c**. This mixture was carried through the sequence yielding compounds **8c** and **8d**, which were separable by preparative HPLC. The reagents and conditions are specified in Scheme 1.

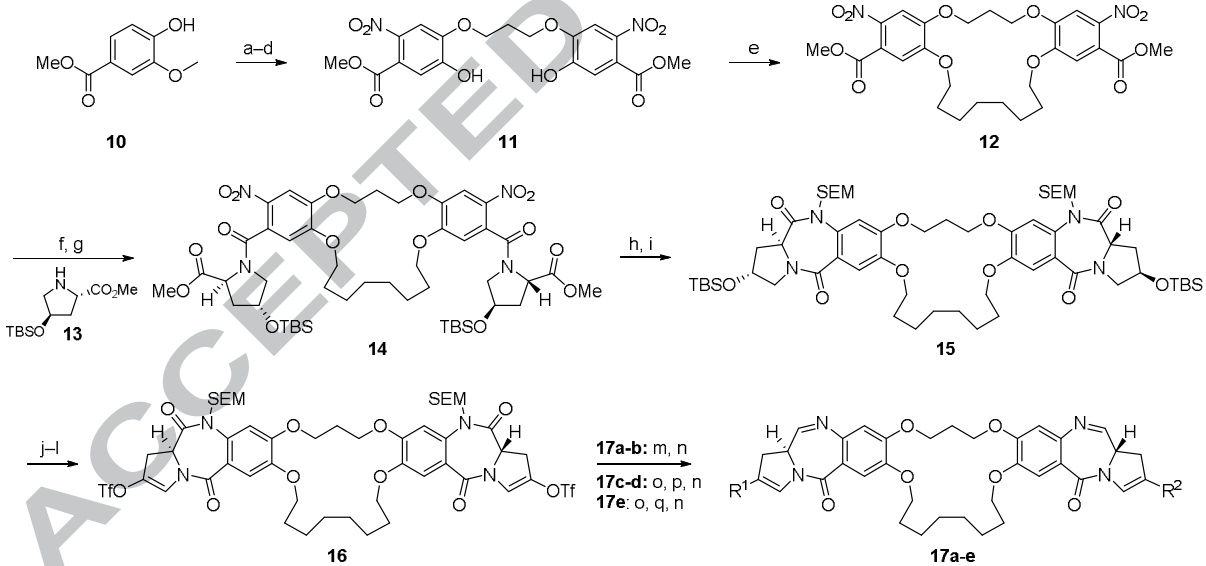

Scheme 3. Reagents and conditions: (a) 1,3-dibromopropane, K_2CO_3, DMSO, rt, 52%; (b) $SnCl_4$, HNO_3, CH_2Cl_2, –25 °C, 82%; (c) NaOH, H_2O, 100 °C, 96%; (d) $(COCl)_2$, cat. DMF, THF, rt; MeOH, 97%; (e) 1,8-diiodooctane, K_2CO_3, DMF, 100 °C, 47%; (f) NaOH, H_2O, MeOH, 50 °C, 95%; (g) $(COCl)_2$, cat. DMF, THF, rt; **13**, Et_3N, THF, 0 °C, 96%; (h) Zn, NH_4Cl, MeOH, THF, 50 °C, quant.; (i) NaH, DMF, 0 °C; SEMCl, 76%; (j) TBAF, THF, rt, 93%; (k) SO_3•pyr., Et_3N, DMSO, CH_2Cl_2, 0 °C to rt, 81%; (l) Tf_2O, 2,6-lut., CH_2Cl_2, –78 °C to –20 °C, 65%; (m) $RB(OH)_2$ (2.2 equiv), $PdCl_2(dppf)$, aq. K_3PO_4, THF, rt; (n) $LiBHEt_3$, THF, –78 °C; silica gel, $CHCl_3$, EtOH, H_2O; (o) (4-aminophenyl)boronic acid pinacol ester (1.0 equiv), $PdCl_2(dppf)$, aq. K_3PO_4, THF, rt, 42%; (p) $R^2B(OH)_2$ (1.1 equiv), $PdCl_2(dppf)$, aq. K_3PO_4, THF, rt; (q) MeMgBr, $Fe(acac)_3$, 20:1 NMP–THF, –30 °C, 51%.

The activity of the C2-unsubstituted macrocycles **8a–f** is summarized in Table 1. As a direct comparator, we also tested the non-macrocyclic analog **9**.[17] Inhibitory activity was measured against three cancer cell lines using a cell proliferation assay. Consistent with our modeling, macrocyclization was tolerated, and substantial improvements in potency were noted with several of the macrocyclic analogs compared with **9**. An 8-carbon chain provided the optimal ring size (compound **8b**).

Table 1. Cell proliferation inhibitory data for C2-unsubstituted macrocycles **8a–f** versus non-macrocyclic comparator **9**

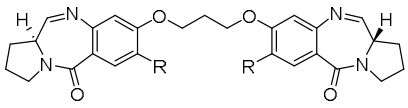

8–9

Cmpd	R	IC_{50} (nM)[a]		
		H226	N87	OVCAR3
9	–OMe	70	63	56
8a	$–O(CH_2)_7O–$	8.1	4.6	3.4
8b	$–O(CH_2)_8O–$	1.6	2.7	1.2
8c	$–O(CH_2)_9O–$	8.7	8.3	7.3
8d	$–O(CH_2)_{10}O–$	12	22	20
8e	$–O(CH_2)_{11}O–$	69	146	78
8f	$–O(CH_2)_{12}O–$	109	306	136

[a]Activity was measured using an MTS cell proliferation assay following 72 h incubation with the test compound.

The combination of C2-substitution and unsaturation typically increases the cytotoxicity of PBDs. For example, the non-macrocyclic compound **19**, which has an endocyclic olefin with phenyl substitution at C2, displayed a >400-fold improvement in potency compared with **9** (Table 2). Interestingly, introduction of these features onto our macrocyclic series did not provide the expected potency boost: The 4-methoxyphenyl-substituted macrocycle **17a** showed essentially the same level of activity as its C2-unsubstituted/saturated parent **8b**. Further profiling of **17a** showed that it had poor aqueous solubility (<1 µg/mL at pH 5.5), and we suspected that this was limiting its activity in our assays. In addition to the three cell lines highlighted earlier, we also recorded activity against HCT116 colon cancer cells and a related P-gp-overexpressing HCT116/VM46 cell line. P-gp expression has been linked with reduced activity for some PBD dimers,[18,19] although sensitivity to this mechanism depends on the specific structural features.[I0] In the case of **17a**, potency was attenuated in the drug resistant cell line.

We explored several avenues for improving the solubility of the macrocyclic analogs. For example, the non-macrocyclic compound **19** has a clogP of 5.1. Addition of the lipophilic hydrocarbon linker raises the clogP by two orders of magnitude (for **17a**, the clogP is 7.0). To counter this, we prepared an analog with an ethylene glycol-derived linker (**18**). While this change restored the clogP to the desired level (4.9), solubility remained poor (<1 µg/mL), and there was no substantial impact on the biological activity. As an alternate approach to improving the solubility, we introduced solubilizing groups at the *para*-position of the C2-phenyl rings. In an analogous manner to the work of Howard, et al.,[12,20,21] we introduced 4-methylpiperazine groups (compound **17b**), and we saw a dramatic improvement in both solubility and potency: the aqueous solubility of **17b** was >698 µg/mL (pH 5.5), and this compound had excellent activity, with IC_{50}'s below 100 pM in four of the cell lines.

While the symmetrical homodimer **17b** met our potency criterion, it lacked a suitable handle for linker attachment to allow us to further evaluate it as an ADC payload. Therefore, we prepared heterodimer **17c**, where we replaced one of the 4-(4-methylpiperazine)phenyl groups with an aniline. This compound retained the very high levels of potency seen with **17b**. Notably, this analog also maintained activity against the drug resistant HCT116/VM46 cells.

Varying the R^3 substituent allowed us to tune the potency of the compounds, as shown with analogs **17d** and **17e**. We felt that progressing a suite of payloads with a range of potency levels would allow us to better understand the balance of activity and tolerability in the context of the full ADCs.

Table 2. Cell proliferation inhibitory data for C2-substituted macrocycles **17a-e** and **18** versus non-macrocyclic comparator **19**

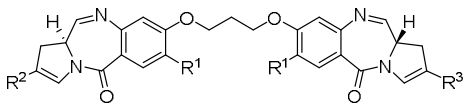

17–19

Compd	R^1	R^2	R^3	IC_{50} (nM)[a]				
				H226	N87	OVCAR3	HCT116	HCT116/VM46
19	–OMe			0.117	0.152	0.126	NT	NT
17a	$–O(CH_2)_8O–$	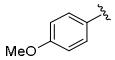	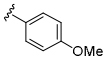	0.993	0.621	1.82	0.167	1.05
18	$–O(CH_2CH_2O)_3–$			1.07	1.54	1.70	0.129	6.44
17b	$–O(CH_2)_8O–$	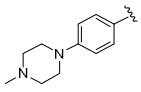	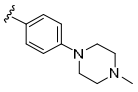	0.047	0.034	0.35	0.006	0.076
17c	$–O(CH_2)_8O–$	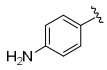	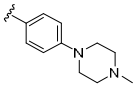	0.024	0.486	0.385	0.016	0.015
17d	$–O(CH_2)_8O–$	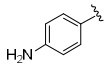	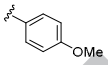	0.355	0.559	0.311	0.063	0.36
17e	$–O(CH_2)_8O–$	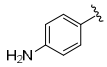		0.655	1.36	1.24	0.135	1.22

[a]Activity was measured using an MTS cell proliferation assay following 72 h incubation with the test compound.

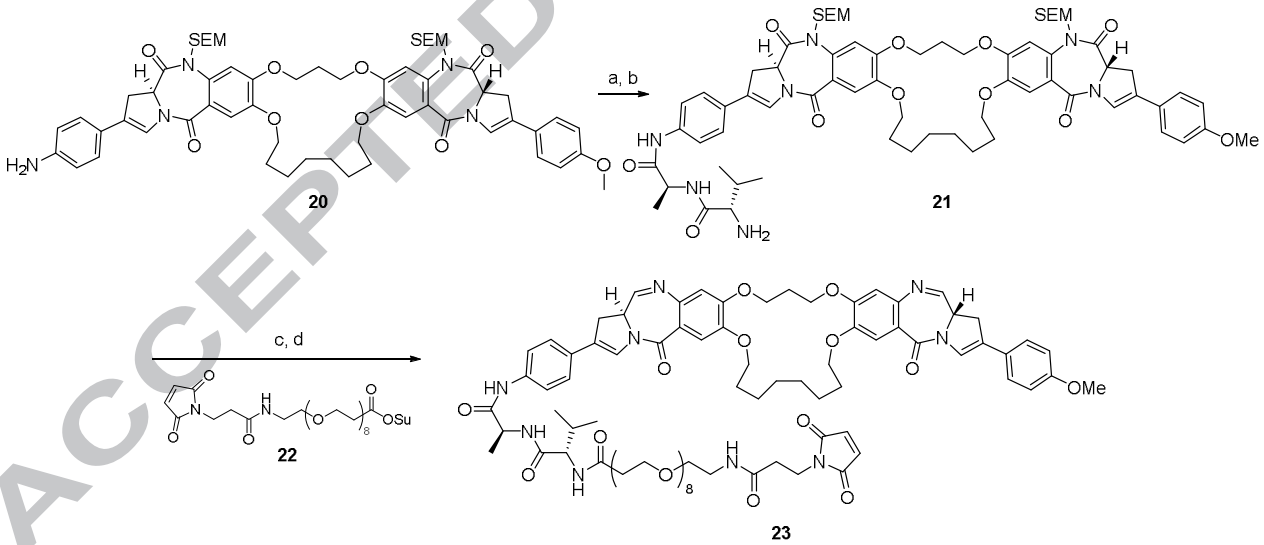

Scheme 4. Reagents and conditions: (a) Fmoc-Val-Ala-OH, HATU, 2,6-lutidine, DMF, rt; (b) piperidine, THF, rt, 85% (2 steps); (c) $LiBHEt_3$, THF, –78 °C; HCO_2H, 1:1:1 THF–MeCN–H_2O, 68%; (d) **22**, 2,6-lutidine, DMSO, rt, 37%.

To evaluate these compounds as ADCs, we installed cathepsin B cleavable valine-alanine linkers and prepared conjugates. This effort is summarized for macrocyclic analog **17d**. Coupling of aniline **20** with Fmoc-Val-Ala-OH was followed by Fmoc deprotection, providing **21** (Scheme 4). Subsequent conversion of the SEM-amides to imines and coupling with the maleimide-containing activated ester **22** completed the synthesis of payload-linker compound **23**. The maleimide group is the thiol-reactive site for antibody conjugation, and the short PEG spacer was included in **22** to balance the lipophilicity of the payload. We assessed the serum stability of this compound, and no free

payload was observed in mouse, rat, or human serum over an incubation period of 24 h.

We conjugated **23** to an antibody targeting mesothelin, a cell-surface glycoprotein that is highly expressed in many cancers,[22] and we measured inhibitory activity against the mesothelin-positive N87 gastric cancer cell line. This cell line does not express CD70, so anti-CD70 conjugates were prepared as isotype controls. Conjugation was effected via thiolated lysine residues: the antibody was treated with 2-iminothiolane to introduce free thiol groups by modification of the ε-amine of lysine residues, and subsequent treatment with **23** led to the isolation of anti-mesothelin-**23** in 78% yield with low levels of aggregation and a drug-antibody ratio (DAR) of 2.5. Similarly, anti-CD70-**23** was obtained in 72% yield with a DAR of 2.2.

The in vitro activity of anti-mesothelin-**23** and anti-CD70-**23** against N87 cells is displayed in Figure 3a. The anti-mesothelin ADC exhibited potent cell growth inhibition (EC_{50} = 0.049 nM). The anti-CD70 ADC control was 90-fold less active (EC_{50} = 4.4 nM). In 786-0 cells (Figure 3b), which are CD70-positive and mesothelin-negative, stong activity was seen with the anti-CD70 ADC (EC_{50} = 0.079 nM), whereas the anti-mesothelin ADC was 190-fold less active (EC_{50} = 15 nM). These data suggest that the observed differential activity derives primarily from antigen-specific processes.

In summary, the high levels of potency and specificity observed with conjugates of **23** illustrate the potential of macrocyclic PBD dimers as novel ADC payloads. While the increased lipophilicity of the macrocyclic compounds presented some challenges, combinations with optimal C2-substituents produced potent analogs that enabled us to demonstrate ADC activity. Additional studies of the therapeutic possibilities of this class of highly-potent DNA modifying agents are ongoing.

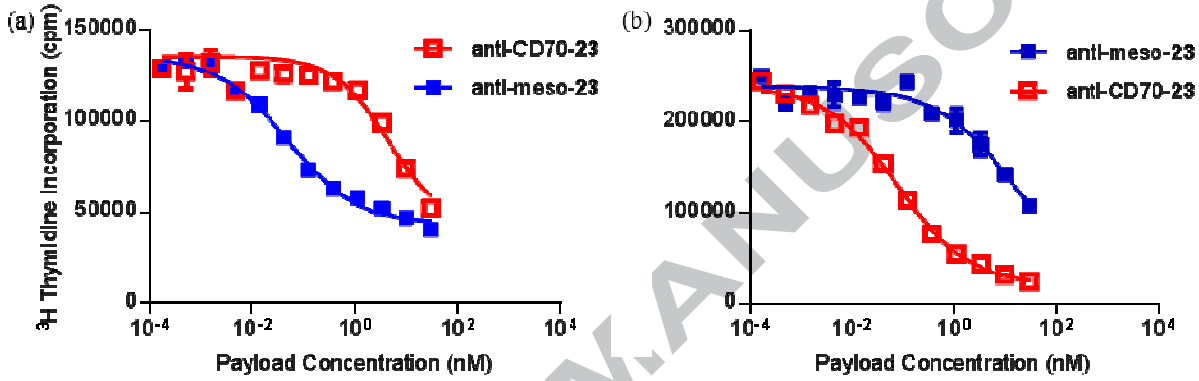

Figure 3. Inhibitory activity of ADCs of PBD macrocycle **23** in (a) N87 gastric cancer cells, and (b) 786-0 cells.

References and notes

1. Perez, H. L.; Cardarelli, P. M.; Deshpande, S.; Gangwar, S.; Schroeder, G. M.; Vite, G. D.; Borzilleri, R. M. *Drug Discovery Today* **2014**, *19*, 869.
2. Chari, R. V. J.; Miller, M. L.; Widdison, W. C. *Angew. Chem. Int. Ed.* **2014**, *53*, 3796.
3. Mantaj, J.; Jackson, P. J.; Rahman, K. M.; Thurston, D. E. *Angew. Chem. Int. Ed.* **2016**, *55*, 2.
4. Hartley, J. A. *Expert Opin. Investig. Drugs* **2011**, *20*, 733.
5. Cipolla, L.; Araújo, A. C.; Airoldi, C.; Bini, D. *Anti-Cancer Agents Med. Chem.* **2009**, *9*, 1.
6. Rahman, K. M.; Thompson, A. S.; James, C. H.; Narayanaswamy, M.; Thurston, D. E. *J. Am. Chem. Soc.* **2009**, *131*, 13756.
7. Sutherland, M. S. K.; Walter, R. B.; Jeffrey, S. C.; Burke, P. J.; Yu, C.; Kostner, H.; Stone, I.; Ryan, M. C.; Sussman, D.; Lyon, R. P.; Zeng, W.; Harrington, K. H.; Klussman, K.; Westendorf, L.; Meyer, D.; Bernstein, I. D.; Senter, P. D.; Benjamin, D. R.; Drachman, J. G.; McEarchern, J. A. *Blood* **2013**, *12*, 1455.
8. Jeffrey, S. C.; Burke, P. J.; Lyon, R. P.; Meyer, D. W.; Sussman, D.; Anderson, M.; Hunter, J. H.; Leiske, C. I.; Miyamoto, J. B.; Nicholas, N. D.; Okeley, N. M.; Sanderson, R. J.; Stone, I. J.; Zeng, W.; Gregson, S. J.; Masterson, L.; Tiberghien, A. C.; Howard, P. W.; Thurston, D. E.; Law, C.-L.; Senter, P. D. *Bioconjugate Chem.* **2013**, *24*, 1256.
9. Tiberghien, A. C.; Levy, J.-N.; Masterson, L. A.; Patel, N. V.; Adams, L. R.; Corbett, S.; Williams, D. G.; Hartley, J. A.; Howard, P. W. *ACS Med. Chem. Lett.* **2016**, *7*, 983.
10. Dubowchik, G. M.; Firestone, R. A.; *Bioorg. Med. Chem. Lett.* **1998**, *8*, 3341.
11. Dubowchik, G. M.; Firestone, R. A.; Padilla, L.; Willner, D.; Hofstead, S. J.; Mosure, K.; Knipe, J. O.; Lasch, S. J.; Trail, P. A. *Biooconjugate Chem.* **2002**, *13*, 855.
12. Antonow, D.; Kaliszczak, M; Kang, G.-D.; Coffils, M.; Tiberghien, A. C.; Cooper, N.; Barata, T.; Heidelberger, S.; James, C. H.; Zloh, M.; Jenkins, T. C.; Reszka, A. P.; Keidle, S.; Guichard, S. M.; Jodrell, D. I.; Hartley, J. A.; Howard, P. W.; Thurston, D. E. *J. Med. Chem.* **2010**, *53*, 2927.
13. Wells, G.; Martin, C. R. H.; Howard, P. W.; Sands, Z. A.; Laughton, C. A.; Tiberghien, A.; Woo, C. K.; Masterson, L. A.; Stephenson, M. J.; Hartley, J. A.; Jenkins, T. C.; Shnyder, S. D.; Loadman, P. M.; Waring, M. J.; Thurston, D. E. *J. Med. Chem.* **2006**, *49*, 5442.
14. Hong, S. H.; Sanders, D. P.; Lee, C. W.; Grubbs, R. H. *J. Am. Chem. Soc.* **2005**, *127*, 17160.
15. Mori, M.; Uozumi, Y.; Kimura, M.; Ban, Y. *Tetrahedron* **1986**, *42*, 3793.
16. Buckman, B.; Nicholas, J. B.; Serebryany, V.; Seiwert, S. D. Patent WO 2012040242, **2012**.
17. Bose, D. S.; Thompson, A. S.; Ching, J.; Hartley, J. A.; Berardini, M. D.; Jenkins, T. C.; Neidle, S.; Hurley, L. H.; Thurston, D. E. *J. Am. Chem. Soc.* **1992**, *114*, 4939.
18. Guichard, S. M.; Macpherson, J. S.; Thurston, D. E.; Jodrell, D. I. *Eur. J. Cancer* **2005**, *41*, 1811.
19. Aird, R. E.; Thomson, M.; Macpherson, J. S.; Thurston, D. E.; Jodrell, D. I., Guichard, S. M. *Pharmacogenomics J.* **2008**, *8*, 289.
20. Howard, P. W.; Van Berkel, P. H. C. Patent WO 2015052533, **2015**.
21. Howard, P. W.; Tiberghien, A.; Cailleau, T. Patent WO 2015052321, **2015**.
22. Hassan, R.; Ho, M. *Eur. J. Cancer* **2008**, *44*, 46.

Supplementary Data

Supplementary data associated with this article can be found in the online version.